ORIGINAL ARTICLE

Fusion of MRIs and CT Scans for Surgical Treatment of Cholesteatoma of the Middle Ear in Children

Isabelle Plouin-Gaudon, MD; Denis Bossard, MD; Sonia Ayari-Khalfallah, MD; Patrick Froehlich, MD, PhD

Objective: To evaluate the efficiency of diffusion-weighted magnetic resonance imaging (MRI) and high-resolution computed tomographic (CT) scan coregistration in predicting and adequately locating primary or recurrent cholesteatoma in children.

Design: Prospective study.

Setting: Tertiary care university hospital.

Patients: Ten patients aged 2 to 17 years (mean age, 8.5 years) with cholesteatoma of the middle ear, some of which were previously treated, were included for follow-up with systematic CT scanning and MRI between 2007 and 2008.

Interventions: Computed tomographic scanning was performed on a Siemens Somaton 128 (0.5/0.2-mm slices reformatted in 0.5/0.3-mm images). Fine cuts were obtained parallel and perpendicular to the lateral semicircular canal in each ear (100 × 100-mm field of view). Magnetic resonance imaging was undertaken on a Siemens Avanto 1.5T unit, with a protocol adapted for young children. Diffusion-weighted imaging was acquired using a single-shot turbo spin-echo mode. To allow for diagnosis and localization of the cholesteatoma, CT and diffusion-weighted MRIs were fused for each case.

Results: In 10 children, fusion technique allowed for correct diagnosis and precise localization (hypotympanum, epitympanum, mastoid recess, and attical space) as confirmed by subsequent standard surgery (positive predictive value, 100%). In 3 cases, the surgical approach was adequately determined from the fusion results. Lesion sizes on the CT-MRI fusion corresponded with perioperative findings.

Conclusions: Recent developments in imaging techniques have made diffusion-weighted MRI more effective for detecting recurrent cholesteatoma. The major drawback of this technique, however, has been its poor anatomical and spatial discrimination. Fusion imaging using high-resolution CT and diffusion-weighted MRI appears to be a promising technique for both the diagnosis and precise localization of cholesteatomas. It provides useful information for surgical planning and, furthermore, is easy to use in pediatric cases.

Arch Otolaryngol Head Neck Surg. 2010;136(9):878-883

Author Affiliations:
Department of Otolaryngology and Head and Neck Surgery, Centre Hospitalier de Valence, Valence, France (Dr Plouin-Gaudon); Department of Radiology, Hôpital Privé Jean Mermoz, Lyon, France (Dr Bossard); and Department of Pediatric Otolaryngology and Head and Neck Surgery, Hôpital Femme-Mère-Enfant, Bron, France (Drs Ayari-Khalfallah and Froehlich).

RECURRENT, RESIDUAL, AND congenital cholesteatomas may prove to be a surveillance and diagnostic challenge. Surgery remains the only possible means of obtaining a clear-cut diagnosis. For this reason, over the past years, several radiology and ear, nose, and throat (ENT) teams have adapted new imaging techniques to visualize cholesteatomas within the middle ear cavities. Computed tomography (CT) is still considered the gold standard of middle ear imaging, even for cholesteatomas, because of its excellent spatial resolution and delineation of strategic anatomical landmarks.[1-4] However, as mentioned in prior studies, one of the main disadvantages of CT is the low specificity with regard to differentiating cholesteatoma from other soft tissue whenever the middle ear appears partially or completely opacified.[5] In previously operated ears, such situations may arise in 20% to 30% of cases.[1,6-10]

Rapid and recent developments of MRI, as well as its more widespread use over the past 10 years, have made it an attractive and promising tool for cholesteatoma diagnosis. Initial studies by Williams et al[1] and Ayache et al[7] advocated the use of MRI with delayed-contrast T1-weighted sequences, for their high specificity, even in case of small lesions (down to 2 mm). More recently, diffusion-weighted techniques have shown promising results in differentiating cholesteatoma from granulation tissue.[3,4,8,10-16] This technique has the advantage of being rapid and convenient. It does not necessitate the injection of contrast material. According to Venail et al,[16] it has nonetheless a high specificity for cholesteatomas as small as 5 mm and shows excellent interobserver agreement.

We found that diffusion-weighted MRI could depict cholesteatomas as small as 3 mm.[17] Moreover, the technique, owing to its short imaging time, seemed well adapted for pediatric cases. Taking these advantages into consideration, and with the idea of trying to increase diffusion-weighted MRI imaging specificity and anatomical location for cholesteatomas, we decided to prospectively evaluate the fusion of CT scans and diffusion-weighted MRI images, in children with strongly suspected residual or congenital cholesteatomas. To our knowledge, this is the first report of fusing CT scans and diffusion-weighted MRI images in this particular setting.

METHOD

PATIENTS

Ten patients, 2 girls and 8 boys, aged 2 to 17 years (mean age, 8.5 years), were prospectively included in our prospective study between 2007 and 2008. Eight had a medical history of cholesteatoma, with 1 or more attempts at surgical removal, and were referred to the tertiary care pediatric ENT center. In the majority of cases, initial surgery consisted in a canal wall up procedure. Only 1 patient had already necessitated a canal wall down technique because of extensive cholesteatoma. All patients had unilateral cholesteatoma. Hence, a total of 10 ears were analyzed.

Inclusion criteria were as follows: age 18 years or younger, history of middle ear surgery for cholesteatoma or strong suspicion of congenital cholesteatoma, follow-up in the same outpatient clinic, second-look surgery programmed in cases of suspected recurrence, and CT and MRI performed prior to revision surgery.

Recorded data included the following: patient age and sex, relevant otologic history, previous surgical procedures for cholesteatoma, dates of last interventions, dates and results of CT scan and MRI, imaging technique, and results of last ear surgery.

IMAGING PROTOCOLS

High-Resolution CT

High-resolution CT was performed on a 128-row multislice scanner (Somatom AS 128; Siemens, Erlangen, Germany) using an axial volume scan (0.4/0.1-mm slices) with coronal and axial reformations (0.4/0.3 mm; parallel and perpendicular to the lateral semicircular canal), for each ear, and a field of view (FOV) of 100 × 100 mm. Acquisition time was 17.4 seconds, with delivered radiation doses of 147 mGy per patient (parameters: 450 mA, 140 kV).

Magnetic Resonance Imaging

In all 10 cases, MRI was undertaken on an Avanto 1.5T (Siemens) unit using a 16-channel head coil. The following protocol was used: 3-mm coronal fast spin-echo T2-weighted slices (time to recovery [TR], 3510 milliseconds [ms]; time to echo [TE], 110 ms; flip angle, 150°; FOV, 230 mm; and number of acquisitions, 1); 0.5-mm axial highly weighted T2 (constructive interference steady-state) transverse slices (TR, 11.89 ms; TE, 5.95 ms; flip angle, 80°; FOV, 200 mm; and number of acquisitions, 1); and 3-mm transverse diffusion ($b = 1000$ s/mm^2)–weighted images with single-shot fast T2 (half-Fourier acquisition single-shot turbo spin-echo [HASTE]) (TR, 1900 ms; TE, 110 ms; flip angle, 172°; FOV, 200 mm; and number of acquisitions, 15). No apparent diffusion coefficient map was established, as only B1000 images were taken into consideration, with the imaging protocol that had been chosen for the study. The goal was to picture only lesions that appear the most hyperintense on B1000 sequences, which offer more relative restriction.

There was no interslice gap on diffusion-weighted imaging sequences. No anesthesia nor intravenous contrast media injection was used. All MRI examinations were performed without motion artifacts and were well tolerated throughout the entire take-up time.

Coregistration of CT scans and diffusion-weighted MRIs was performed on a Syngo workstation (Siemens) using the Siemens Image Fusion software. The multimodality commercial imaging software is routinely used in positron emission tomography imaging and radiotherapy. Images from CT and MRI are automatically fused in a hybrid data set, even if slice thickness and FOV are not similar. Degree of opacity and color matches of these overlayed new images may then be set manually.

IMAGING INTERPRETATION

All imaging, whether CT or MRI, was prospectively interpreted by the same radiologist (D.B.), specifically trained in head and neck, and particularly otologic, radiology. On CT, cholesteatoma was diagnosed by identifying a rounded tissue mass in the middle ear cavities, or a mass associated with bone erosion (including the tegmen), ossicular chain amputation, prosthesis displacement, or labyrinthine or facial nerve sheath destruction that could not be attributed to past surgery. Images were considered negative for cholesteatoma when middle ear cavities were either air filled or showed minimal thickening. Interpretation was indicated as being indeterminate, whenever diffuse opacity appeared within the middle ear cavities.

On MRI sequences, the diagnosis of cholesteatoma was based on identifying a hyperintense image on the B1000 images of diffusion-weighted HASTE sequences.

The radiologist classified MRI results as being either positive or negative for cholesteatoma. Tumor dimension at maximum diameter on axial and coronal planes was also recorded on MRI and, when possible, CT.

Fusion of CT scans and diffusion-weighted MRIs allowed precise interpretation of initial MRI results with regard to adequate anatomical location. The fusion image results were then compared with surgical findings.

RESULTS

The median interval between the last 2 surgical procedures (excluding the 2 cases of initial surgery for congenital cholesteatoma) was 11 months (range, 6-38 months). Computed tomographic scanning and MRI were performed within a median of 5 and 3 weeks, respectively, prior to surgery, ranging from 1 to 15 weeks.

Of the 10 cases included, 9 turned out positive for a cholesteatoma, with 7 residual and 2 congenital lesions. The mean cholesteatoma size was 1 cm, ranging from 3 to 26 mm.

The CT scan was interpreted as positive in 4 cases, 3 of which were also found to be positive during surgery. Six CT scans were considered indeterminate because of complete opacification of the middle ear cavities, without evidence of bony erosion other than modifications imputable to previous operations. None of the CT scans could eliminate the presence of a cholesteatoma.

Table 1. Comparison of CT Scan, MRI, Fusion, and Surgical Findings

Patient No.	CT Scan–Surgery Interval, wk	MRI–Surgery Interval, wk	CT Scan Results	Diffusion-Weighted Non-EPI MRI Results (b=1000 s/mm^2)	CT-MRI Fusion (Results Detailed for Small Cholesteatoma)	Surgical Findings
1	5	1	CO	15-mm Highlighted mass	Full hypotympanum mass	+ Hypotympanum
2	6	6	CO	18-mm Mass	Attical mass	+ Attical
3	4	4	5-mm Nodule hypotympanum	4.5-mm Mass in hypotympanum	4-mm Mass in hypotympanum, no contact with promontory	+ Small cholesteatoma anterior hypotympanum, above promontory
4	10	6	PO	15-mm Mass	Antrum and attic	+ Antrum and attic
5	15	15	6-mm Nodule	–	–	–
6	3	1	CO	19-mm Mass	Mastoid and attical	+ Mastoid and around ossicles
7	1	1	CO	<3-mm Attical mass	3-mm Mass on stapes	+ 3-mm Cholesteatoma around stapes
8	4	1	2 Nodules	12-mm Mass in antrum + mastoid	Attical and partial mastoid	+ Extensive attical and mastoid cholesteatoma
9	1.5	1.5	CO	Extensive highlighted mass	Antrum, attic, mastoid	+ Extensive cholesteatoma, antrum to mastoid
10	5	5	CO	26-mm Mass	Complete middle ear cholesteatoma	+ Extensive cholesteatoma

Abbreviations: CO, complete opacification; CT, computed tomographic; EPI, echoplanar imaging; MRI, magnetic resonance imaging; PO, partial opacification; –, negative finding; +, positive finding.

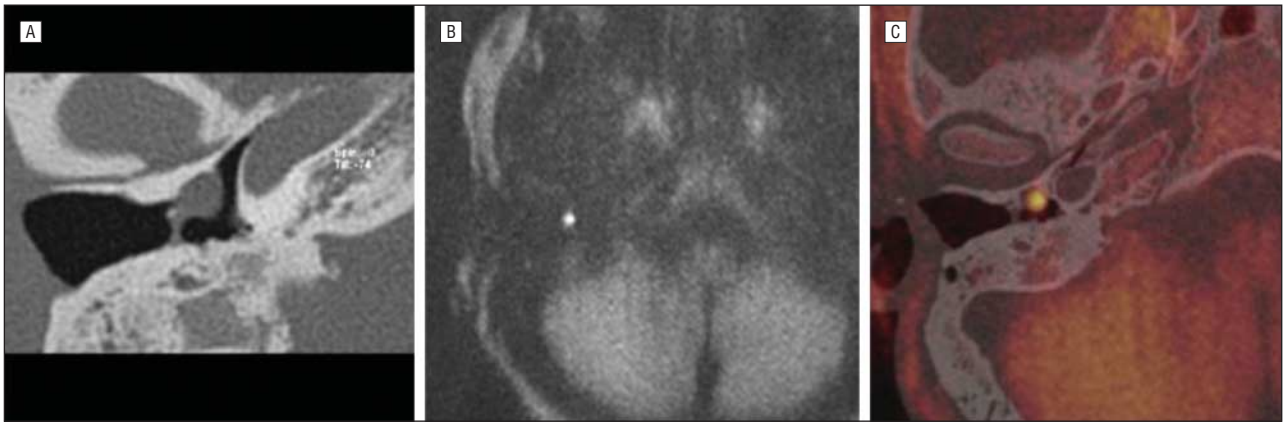

Figure 1. A 17-year-old girl with a history of cholesteatoma, third relapse (last recurrence: 4 years prior to current status). A, Computed tomographic (CT) scan: 5-mm opacity in the hypotympanum, highly suggestive of cholesteatoma; B, non–echoplanar imaging, diffusion-weighted magnetic resonance image (MRI): 4.5-mm highlighted mass in the middle ear; and C, CT and MRI fusion: 4-mm rounded mass, strictly confined in the hypotympanum above the promontory.

Preoperative MRI suggested residual cholesteatoma in 7 cases and congenital cholesteatoma in 2. All of these were confirmed as positive during surgery. There were no false-positive cases, and the smallest cholesteatoma diagnosed on MRI measured 3 mm in its greatest diameter. This was also corroborated by surgical findings. The negative MRI case was confirmed as such during surgery. Thus, the sensitivity and specificity of the non–echoplanar imaging (EPI) diffusion-weighted MRI technique used in this protocol were both 100%.

The results of CT scan and MRI fusion led to a clear diagnosis of a highlighted lesion, precisely located within the middle ear cavities, whenever a cholesteatoma was present (**Table 1**). No anatomical distortions were observed on CT scan and MRI coregistration.

It was possible to determine the exact anatomical site of the lesion, particularly in cases of small cholesteatoma (**Figure 1** and **Figure 2**). In patient 3 (Figure 1), the cholesteatoma was confirmed by the fusion images as situated in the hypotympanum, without direct contact with the promontory. In patient 7 (Figure 2), a 3-mm cholesteatoma was precisely described as located on the promontory, in place of the stapes. In these 2 cases, the surgical approach was therefore limited to a minimal endaural approach, and local findings corroborated precisely with the fusion descriptions. The limited technique proved sufficient for second-look surgery in these cases. In another case (patient 9; **Figure 3**), the surgical approach was, on the contrary, expanded because of apparent massive extension into the mastoid, which proved to be a fruitful adaptation. Perioperative findings confirmed the exact anatomical descriptions of cholesteatomas as reported on fusion images in all cases.

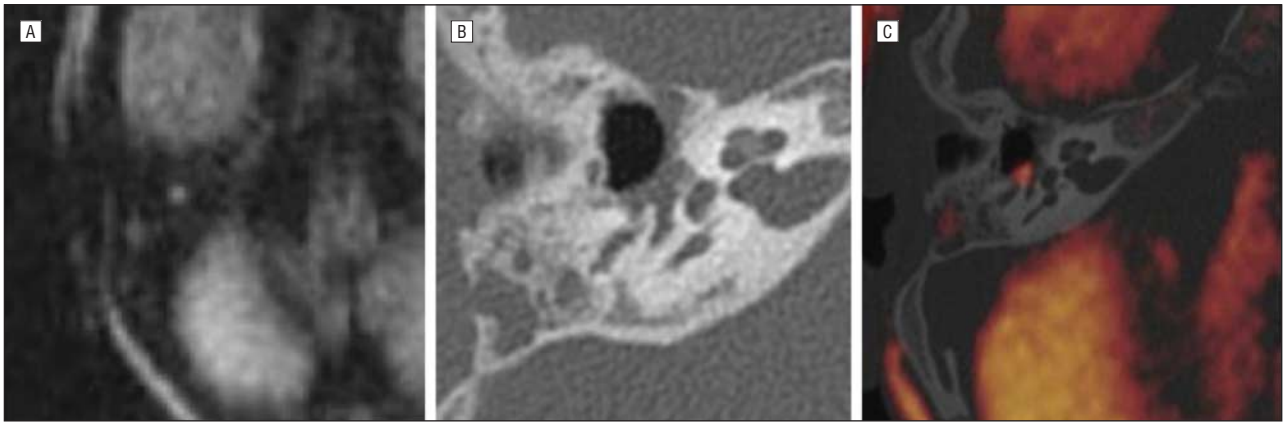

Figure 2. A 5-year-old boy, first cholesteatoma recurrence (previous episode 6 months prior to current status). A, Computed tomographic (CT) scan: opacification of mastoid and majority of middle ear; B: non–echoplanar imaging, diffusion-weighted magnetic resonance image (MRI): 3-mm highlighted mass within the middle ear; and C, CT and MRI fusion: 3-mm mass on the promontory in place of the stapes.

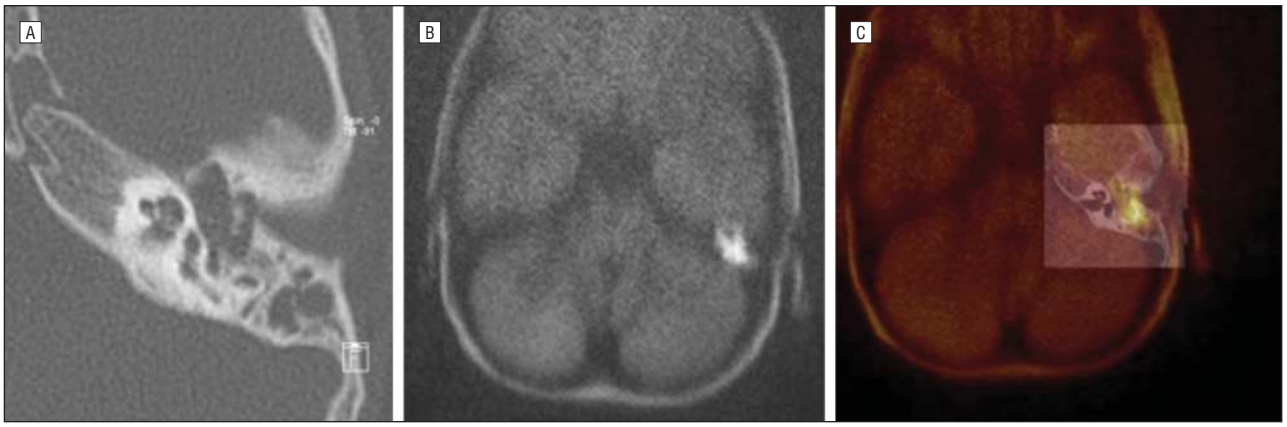

Figure 3. A 2-year-old boy with congenital cholesteatoma. A, Complete middle ear and mastoid opacification; B, large highlighted mass probably within the middle ear; and C, computed tomography and magnetic resonance image fusion: large mass filling the antrum, attical space and mastoid.

COMMENT

Although great progress has recently been accomplished with MRI techniques, no single imaging technique stands out as perfectly able to confirm or rule out the presence of a cholesteatoma, especially in the case of a residual lesion. High-resolution CT scanning still remains the gold standard for postoperative middle ear assessment.[10] It has the advantage of precisely delineating anatomical structures and landmarks and offers the possibility of multiplanar reconstruction. In certain situations, when it reveals a single, rounded middle ear opacity, with adjacent bony erosion, a diagnosis of cholesteatoma may readily be suggested. However, differentiating cholesteatoma from other surrounding soft tissue, such as inflammation, scar tissue or middle ear effusion, is impossible. Even contrast-enhanced CT studies may not be beneficial.[7]

In the present study, most CT scans were considered indeterminate regarding cholesteatoma diagnosis because of the impossibility of distinguishing it from other types of mucosal lesions. We did not determine the sensitivity and specificity of CT scan results as this was not the goal of the study. Rather, the CT scan served as an anatomical canvas on which to superimpose MRI findings in order to refine the diagnosis.

As opposed to CT scanning, MRI offers a rather poor spatial resolution. However, the great advantage of this imaging technique is its ability to discriminate soft tissue.[5] Initial attempts to use MRI to diagnose cholesteatomas were based on the use of delayed contrast-enhanced T1-weighted sequences (SET1), as described and largely advocated by Williams and Ayache and colleagues.[1,7] This imaging technique differentiates cholesteatoma from surrounding fibrosis or inflammation because cholesteatomas never take up contrast even on late sequences. Although it may reveal cholesteatomas as small as 2.5 mm,[18] the technique is limited by the long duration of the protocol and the need to inject contrast material. For these last reasons, we decided not to use SET1 sequences, since they did not seem suitable for children. Although gadolinium injection is routinely used in pediatric cases, we believe that the imaging protocol would be best tolerated and the overall examination duration shorter if all venous punctures, which we consider as being invasive, could be avoided. Increasing the child's tolerance to the procedure to avoid any kind of unnecessary sedation seemed mandatory to us.

Recently, diffusion-weighted MRI has aroused great interest in the radiology and ENT community because of its increased specificity, rapid imaging time, and high

Table 2. Previous Studies on the Use of Diffusion-Weighted MRI for the Evaluation of Recurrent or Residual Cholesteatoma

Source	No. of Patients	MRI Technique	NPV, %	PPV, %	Size Limit
Aikele et al,[4] 2003	17	EPI	100	75	5 mm
Stasolla et al,[6] 2004	18	EPI	92	100	5 mm
Dubrulle et al,[8] 2006	24	Non-EPI	100	93	5 mm
Vercruysse et al,[12] 2006	100	EPI	40-72	100	5 mm
De Foer et al,[10] 2007	21	Non-EPI	100	93	2 mm
Emonot et al,[20] 2008	61	EPI	88	90	3 mm
Venail et al,[16] 2008	31	EPI	50	80	5 mm
Plouin-Gaudon et al,[17] 2008	20 Children	Non-EPI	89	58	3 mm
Dephnorrarat et al,[13] 2009	22	Non-EPI	100	100	3 mm
De Foer et al,[15] 2008	19 Operated	Non-EPI	96	100	2 mm
Plouin-Gaudon et al, 2010 (present study)	10	Non-EPI	100	100	3 mm

Abbreviations: EPI, echoplanar imaging; MRI, magnetic resonance imaging; NPV, negative predictive value; PPV, positive predictive value.

interobserver agreement rate.[16] The technique is based on an imaging mode of free water molecules. A marked hyperintense signal corresponds to a lesion in which molecules are binded, or trapped, such as in a very cohesive cholesteatoma lesion. Controversy remains as to the explanation for this bright signal.[3,4,19] It has been postulated that the high signal shown by cholesteatomas is due to a T2 shine-through effect.[10,12] Because it was initially routinely used for cerebral imaging, diffusion-weighted EPI has been most frequently reported on in the evaluation of residual cholesteatomas.[4,6,12,16,20] The hyperintense signal for a cholesteatoma is most marked and characteristic with a B1000 diffusion coefficient.[8,21] However, susceptibility artifacts and major distortions around the skull base and air-bone interfaces are now well-known limitations of the technique.[8,10,13] Most studies using this technique conclude that the smallest cholesteatoma lesion that may be revealed measures no less than 5 mm[4,6,12,16,20] (**Table 2**).

Dubrulle et al[8] demonstrated in a recent study that non-EPI diffusion-weighted imaging presented far fewer susceptibility artifacts and distortions, thus increasing the spatial resolution of MRIs. However, these results were only compared with contrast-enhanced delayed T1 sequences and not with an EPI technique. Dhepnorrarat et al[13] and De Foer et al[11] compared EPI and non-EPI results with regard to susceptibility artifacts and showed far less cranial base distortion with non-EPI sequences. Such SSTSE (single-shot turbo spin-echo) or HASTE sequences thus enable better localization and differentiation of cholesteatomas from other surrounding soft tissues. In the present study, HASTE diffusion-weighted MRI revealed a cholesteatoma in all true-positive cases. Moreover, no false-positive nor false-negative cases were found. The absence of false-negative cases may have been explained by the fact that none of the cases displayed recurrent cholesteatoma in the form of thin matrix layers. Only small pearls were found. Coregistration of CT scans and diffusion-weighted MRIs also confirmed that there was no cranial base distortion with the non-EPI technique, as images coincided perfectly.

In our initial study (presented at the 2008 American Society of Pediatric Otolaryngology Annual Meeting[17]), we encountered difficulties in visualizing cholesteatomas of 2 or 3 mm in several patients, although this was not attributable to motion artifacts. This could have been owing to the short intersurgery interval and the delay between MRI and the second-look procedure. As opposed to most studies, which mainly included adult patients, our pediatric series imposed a more rigorous follow-up and often rapid second-look surgery because cholesteatomas seem to be more aggressive in children. To increase the congruence between MRI and surgical findings, we were able to limit the delay of preoperative MRIs in most cases to less than 1 month. This may also have contributed to the high negative and positive predictive values found in our diffusion-weighted MRI series, even though only 10 patients have as yet been included. This remains a major flaw in our preliminary report. We realize that although our results seem encouraging, the study lacks statistical power to draw clear-cut conclusions. However, we claim that it demonstrates the feasibility and promising aspect of a novel technique.

We therefore believe it is worth underlining the advantages of fusing high-resolution CT scans and non-EPI diffusion-weighted MRIs for precise localization of cholesteatoma lesions. When superimposing the 2 imaging results, anatomical delineation appears totally congruent and the hyperintense cholesteatoma is clearly situated within the middle ear and mastoid cavities (Figures 1-3). The poor spatial resolution of the MRIs is replaced by the anatomical precision of the CT scan, and the enhancing cholesteatoma becomes strikingly evident even to a nonradiologist. The combination of imaging techniques thus provides a useful tool for the surgeon who can visualize precisely the location of the cholesteatoma and possibly choose a limited approach. This may reduce local complications and lessen operative time. In 3 of our cases, the surgical approach was modified and guided according to image fusion results. After scrupulous surgical evaluation, this adaptation was judged adequate and devoid of any risk of leaving cholesteatoma behind.

Further study of our findings with additional patients is essential to confirm the specificity of high-resolution CT scan and non-EPI diffusion-weighted MRI fusion and the validity of consequently modified surgical approaches for second-look surgery, if not surgical adjournment of, or abstention from, surgery

In conclusion, recent developments in imaging techniques have made diffusion-weighted MRI, particularly

in non-EPI mode, more effective for detecting recurrent cholesteatoma. Thus far, the major drawback of this technique has been its poor anatomical and spatial discrimination. According to our preliminary results, fusion imaging using high-resolution CT and non-EPI diffusion-weighted MRI appears to be a promising technique for both diagnosis and precise localization of cholesteatomas. It provides useful information to the surgeon in planning a surgical intervention and is easy to use for pediatric cases.

Submitted for Publication: March 31, 2009; final revision received January 8, 2010; accepted March 31, 2010.
Correspondence: Patrick Froehlich, MD, PhD, Department of Pediatric Otolaryngology and Head and Neck Surgery, Hôpital Femme-Mère-Enfant, 59 Blvd Pinel, Bron 69677, France (patrick.froehlich@chu-lyon.fr).
Author Contributions: Drs Plouin-Gaudon, Bossard, and Froehlich had full access to all the data in the study and take responsibility for the integrity of the data and the accuracy of the data analysis. *Study concept and design:* Plouin-Gaudon, Bossard, and Froehlich. *Acquisition of data:* Bossard, Ayari-Khalfallah, and Froehlich. *Analysis and interpretation of data:* Plouin-Gaudon and Bossard. *Drafting of the manuscript:* Plouin-Gaudon. *Critical revision of the manuscript for important intellectual content:* Plouin-Gaudon, Bossard, Ayari-Khalfallah, and Froehlich. *Statistical analysis:* Plouin-Gaudon. *Obtained funding:* Bossard. *Administrative, technical, and material support:* Bossard, Ayari-Khalfallah, and Froehlich. *Study supervision:* Plouin-Gaudon, Bossard, and Froehlich.
Financial Disclosure: None reported.
Previous Presentation: This study was presented at the 2009 American Society of Pediatric Otolaryngology Annual Meeting; May 23, 2009; Seattle, Washington.
Additional Contributions: Chantal Giguère, MD, gave suggestions regarding the writing of the manuscript.

REFERENCES

1. Williams MT, Ayache D. Imaging in adult chronic otitis [in French]. *J Radiol*. 2006; 87(11, pt 2):1743-1755.
2. Maroldi R, Farina D, Palvarini L, et al. Computed tomography and magnetic resonance imaging of pathologic conditions of the middle ear. *Eur J Radiol*. 2001; 40(2):78-93.
3. De Foer B, Vercruysse JP, Pilet B, et al. Single-shot, turbo spin-echo, diffusion-weighted imaging versus spin-echo-planar, diffusion-weighted imaging in the detection of acquired middle ear cholesteatoma. *AJNR Am J Neuroradiol*. 2006; 27(7):1480-1482.
4. Aikele P, Kittner T, Offergeld C, Kaftan H, Hüttenbrink KB, Laniado M. Diffusion-weighted MR imaging of cholesteatoma in pediatric and adult patients who have undergone middle ear surgery. *AJR Am J Roentgenol*. 2003;181(1):261-265.
5. Williams MT, Ayache D. Imaging of the postoperative middle ear. *Eur Radiol*. 2004; 14(3):482-495.
6. Stasolla A, Magliulo G, Parrotto D, Luppi G, Marini M. Detection of postoperative relapsing/residual cholesteatomas with diffusion-weighted echo-planar magnetic resonance imaging. *Otol Neurotol*. 2004;25(6):879-884.
7. Ayache D, Williams MT, Lejeune D, Corré A. Usefulness of delayed postcontrast magnetic resonance imaging in the detection of residual cholesteatoma after canal wall-up tympanoplasty. *Laryngoscope*. 2005;115(4):607-610.
8. Dubrulle F, Souillard R, Chechin D, Vaneecloo FM, Desaulty A, Vincent C. Diffusion-weighted MR imaging sequence in the detection of postoperative recurrent cholesteatoma. *Radiology*. 2006;238(2):604-610.
9. Watts S, Flood LM, Clifford K. A systematic approach to interpretation of computed tomography scans prior to surgery of middle ear cholesteatoma. *J Laryngol Otol*. 2000;114(4):248-253.
10. De Foer B, Vercruysse JP, Pouillon M, Somers T, Casselman JW, Offeciers E. Value of high-resolution computed tomography and magnetic resonance imaging in the detection of residual cholesteatomas in primary bony obliterated mastoids. *Am J Otolaryngol*. 2007;28(4):230-234.
11. De Foer B, Vercruysse JP, Pilet B, et al. Single-shot, turbo spin-echo, diffusion-weighted imaging versus spin-echo-planar, diffusion-weighted imaging in the detection of acquired middle ear cholesteatoma. *AJNR Am J Neuroradiol*. 2006; 27(7):1480-1482.
12. Vercruysse JP, De Foer B, Pouillon M, Somers T, Casselman J, Offeciers E. The value of diffusion-weighted MR imaging in the diagnosis of primary acquired and residual cholesteatoma: a surgical verified study of 100 patients. *Eur Radiol*. 2006;16(7):1461-1467.
13. Dhepnorrarat RC, Wood B, Rajan GP. Postoperative non-echo-planar diffusion-weighted magnetic resonance imaging changes after cholesteatoma surgery: implications for cholesteatoma screening. *Otol Neurotol*. 2009;30(1):54-58.
14. Toyama C, Leite CdaC, Baraúna Filho IS, et al. The role of magnetic resonance imaging in the postoperative management of cholesteatomas. *Braz J Otorhinolaryngol*. 2008;74(5):693-696.
15. De Foer B, Vercruysse JP, Bernaerts A, et al. Detection of postoperative residual cholesteatoma with non-echo-planar diffusion-weighted magnetic resonance imaging. *Otol Neurotol*. 2008;29(4):513-517.
16. Venail F, Bonafe A, Poirrier V, Mondain M, Uziel A. Comparison of echo-planar diffusion-weighted imaging and delayed postcontrast T1-weighted MR imaging for the detection of residual cholesteatoma. *AJNR Am J Neuroradiol*. 2008; 29(7):1363-1368.
17. Plouin-Gaudon I, Bossard D, Fuchsmann C, Ayari-Khalfallah S, Froehlich P. Diffusion-weighted MR imaging for evaluation of pediatric recurrent cholesteatomas. *Int J Pediatr Otorhinolaryngol*. 2010;74(1):22-26.
18. Williams MT, Ayache D, Alberti C, et al. Detection of postoperative residual cholesteatoma with delayed contrast-enhanced MR imaging: initial findings. *Eur Radiol*. 2003;13(1):169-174.
19. Maheshwari S, Mukherji SK. Diffusion-weighted imaging for differentiating recurrent cholesteatoma from granulation tissue after mastoidectomy: case report. *AJNR Am J Neuroradiol*. 2002;23(5):847-849.
20. Emonot G, Richard C, Dumollard JM, Veyret C, Martin C. Contribution of MRI to diagnosis of residual cholesteatoma [in French]. *Fr ORL*. 2008;94:366-374.
21. Lemmerling MM, De Foer B, VandeVyver V, Vercruysse JP, Verstraete KL. Imaging of the opacified middle ear. *Eur J Radiol*. 2008;66(3):363-371.